Stratigraphic noise and its potential drivers across the plateau of Dronning Maud Land, East Antarctica

Nora Hirsch[1], Alexandra Zuhr[1], Thomas Münch[1], Maria Hörhold[2], Johannes Freitag[2], Remi Dallmayr[2], and Thomas Laepple[1, 3]

[1]Alfred-Wegener-Institut, Helmholtz Centre for Polar and Marine Research, Potsdam, Germany
[2]Alfred-Wegener-Institut, Helmholtz Centre for Polar and Marine Research, Bremerhaven, Germany
[3]University of Bremen, MARUM – Centre for Marine Environmental Sciences and Faculty of Geosciences, Bremen, Germany

Correspondence: Nora Hirsch (nora.hirsch@awi.de)

Abstract. Stable water isotopologues of snow, firn, and ice cores provide valuable information on past climate variations. Yet single profiles are generally not suitable for robust climate reconstructions. Stratigraphic noise, introduced by the irregular deposition, wind driven erosion and redistribution of snow, impacts the utility of high resolution isotope records, especially in low accumulation areas. However, it is currently unknown how stratigraphic noise differs across the East Antarctic Plateau
5   and how it is affected by local environmental conditions. Here, we assess the amount and structure of stratigraphic noise at seven sites along a 120 km transect on the plateau of Dronning Maud Land, East Antarctica. Replicated oxygen isotope records of 1 m length were used to estimate signal to noise ratios as a measure of stratigraphic noise ~~, while~~ at sites characterised by different accumulation rates (43–64 mm w.eq. ~~a-1~~a^{-1}), snow surface ~~roughness~~ roughnesses and slope inclinations~~gave insights on the local environmental settings~~. While we found a high amount of stratigraphic noise at all sites, there was also
10   a considerable amount of spatial variability. At sastrugi dominated sites, higher stratigraphic noise coincided with higher surface ~~roughness~~roughnesses, steeper slopes, and lower accumulation rates, probably related to increased wind speeds. These results provide a first step to modelling stratigraphic noise and ~~guide future exhibitions in adjusting their sampling strategies to maximise the usage of high resolution isotope records~~ might guide site selection and sampling strategies for future expeditions to improve high resolution climate reconstructions from low accumulation regions.

1   Introduction

15   The East Antarctic ice sheet is a valuable climate archive. Stable water isotopologues of snow, firn, and ice core records store information on past temperature variations (e.g., Jouzel and Masson-Delmotte, 2010; Dansgaard, 1964), especially on past glacial and interglacial periods (EPICA community members, 2004, 2006). However, the interpretation of isotope records at subannual to decadal resolutions is hampered by significant uncertainties (e.g., Casado et al., 2020; Laepple et al., 2018; Münch and Laepple, 2018) which limit the usability of this archive to quantify recent global warming impacts on the Antarctic (Stenni
20   et al., 2017; Jones et al., 2016). Several processes, such as precipitation intermittency (Laepple et al., 2011; Helsen et al., 2005), water vapour exchange and sublimation (e.g., Wahl et al., 2021; Town et al., 2008), and isotopic diffusion (e.g., Laepple

et al., 2018; van der Wel et al., 2015; Johnsen et al., 2000) introduce noise to the isotopic temperature imprint in snow, firn, and ice cores. Additionally, accumulation does not occur as perfectly stratified layers but is affected by irregular depositions

25 as well as ~~aeolian~~ wind driven erosion and redistribution (Zuhr et al., 2021; Picard et al., 2019). These processes introduce a non-climatic variability in the isotope profiles, known as stratigraphic noise (Fisher et al., 1985), which reduces the usability of single isotope profiles for climate reconstructions ~~as they are not representative~~ (e.g., Münch et al., 2016).

While atmospheric circulation, temperature, and precipitation intermittency introduce differences in the isotopic compositions on scales of hundreds of kilometres (Goursaud et al., 2018; Münch and Laepple, 2018), stratigraphic noise has been

30 defined as the uncorrelated part between two or more isotope profiles at local scales (Fisher et al., 1985). ~~Furthermore,~~ Münch et al. (2016) found the decorrelation length of stratigraphic noise to be around 5 to 10 m on the plateau of Dronning Maud Land (DML), which means that the stratigraphic noise in one snow core is independent from the noise of an adjacent profile at a distance of more than 5-10 m.

Stratigraphic noise hampers the extraction and interpretation of climate signals, especially on subannual to decadal scales

35 where accumulation rates are low (e.g., Jones et al., 2014; Karlöf et al., 2006; McMorrow et al., 2002; Sommer et al., 2000). For instance, with accumulation rates ~~in Greenland of~~ of 240-600 mm w.eq. a^{-1} in Greenland, it is possible to extract seasonal and annual signals from the isotopic imprints in firn cores (Vinther et al., 2010). However, with low accumulation rates of 40 to 90 mm w.eq. a^{-1} in DML (Oerter et al., 2000), seasonal snow layers can be completely eroded (Helsen et al., 2005). Accordingly, discrepancies between isotope profiles and observed temperatures are smaller in coastal areas of East Antarctica

40 compared to the drier inland plateau of DML (Helsen et al., 2005). This is further evidenced by the signal to noise ratios (SNRs), which measure the ratio of the common (spatially coherent) isotopic signal over the independent stratigraphic noise: while Fisher et al. (1985) found SNRs between 1.1 and 2.7 (at 140–520 mm w.eq a^{-1}) for annually resolved ice core records from Greenland, Graf et al. (2002) obtained a SNR of only 0.14 on the plateau of DML.

Although several studies have identified stratigraphic noise as a crucial limiting factor for high resolution ice core signal

45 interpretation, it remains unknown how stratigraphic noise differs spatially, e.g., across the East Antarctic Plateau (EAP), and how it is related to local environmental properties like accumulation rate, slope inclination, and surface roughness. Knowledge of ~~these~~ such relationships would allow to optimise the selection of sampling sites for extracting snow and firn cores for the purpose of high-resolution climate reconstructions. Lower stratigraphic noise from optimal sites would enhance the effective resolution on which a climate signal can be extracted (Casado et al., 2018). Furthermore, this knowledge would enable strati-

50 graphic noise to be simulated in proxy system models (Casado et al., 2018; Dolman and Laepple, 2018; Dee et al., 2015). An improved quantitative understanding would also result in more accurate estimates of past climate variability as it would allow us to correct for stratigraphic noise within the spectral domain (e.g., Münch and Laepple, 2018; Laepple et al., 2017). It might further enable the use of replicate cores as a proxy for past surface roughnesses and related wind speeds ~~, as suggested by Barnes et al. (2006)~~ (Barnes et al., 2006).

55 In this study, we use SNRs to quantify stratigraphic noise in high resolution isotope records collected from seven sites in DML (EAP). We relate differences in stratigraphic noise to varying local environmental properties such as slope inclination, surface roughness, and accumulation rate in order to identify potential underlying environmental drivers.
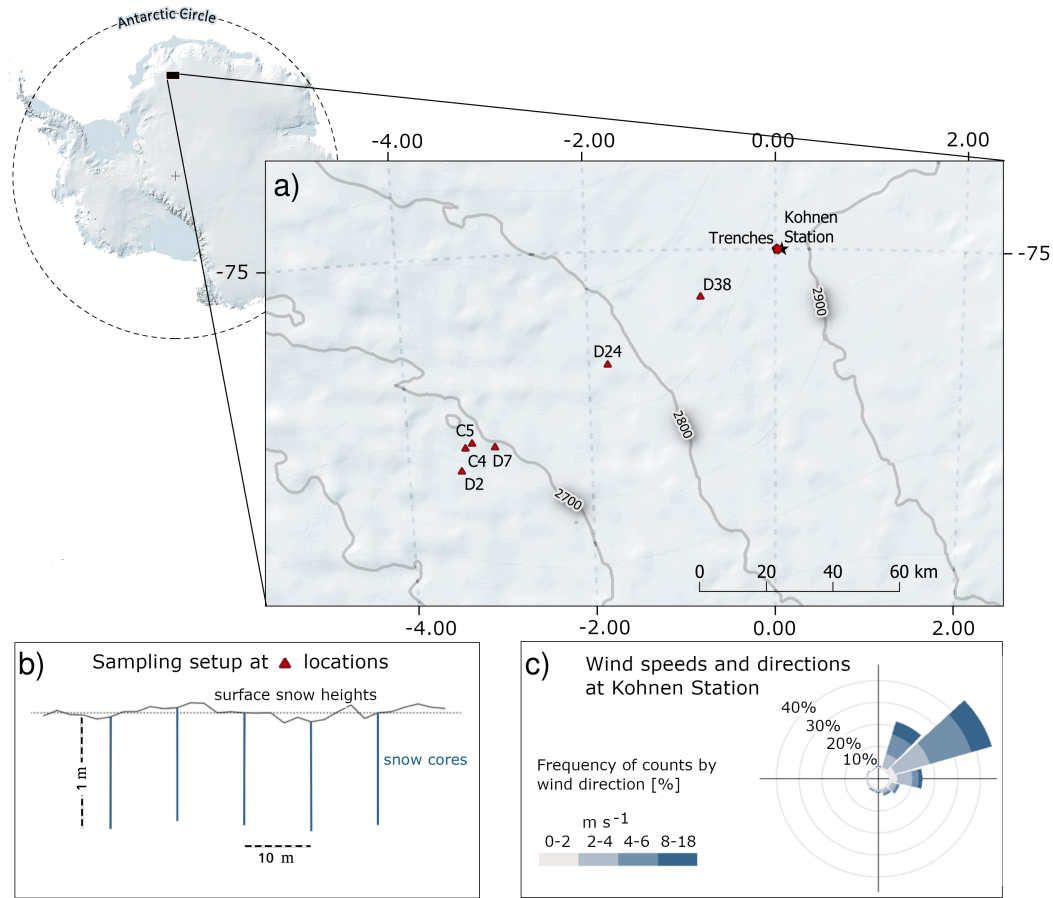
Figure 1. a) Study area on the plateau of Dronning Maud Land (DML), East Antarctica, with sampling sites D2, C4, C5, D7, D24, C38, and Kohnen trenches (Münch et al., 2016, 2017), shading . Shading represent the surface elevation above sea level (RAMP2 Liu et al., 2015). b) Example schematic illustrating the collection of replicate core samples snow cores at each sampling site. c) Wind speeds and direction at Kohnen Station (AWS 9, 2012-2018)(AWS 9, 2012-2018; Reijmer and van den Broeke, 2003).

2 Materials and methods

2.1 Study area

60 The sampling sites are situated on the EAP along a 120 km transect that rises gently from 2685 to 2892 m.a.s.l. near Kohnen Station (Wesche et al., 2016, 75.002°S, 0.007°W, 2892 m.a.s.l.) (75.002°S, 0.007°W, 2892 m.a.s.l.; Wesche et al., 2016) (Fig. 1a). Between 2012 and 2018, the annual mean temperature at Kohnen station was -40.9 °C and the annual mean wind speed was 4.31 m s^{-1} (AWS 9, Reijmer and van den Broeke, 2003). The region is characterized by katabatic winds consistently blowing downslope (e.g., Broeke and Lipzig, 2003; Parish and Cassano, 2003) from north-easterly directions (Fig. 1c), with wind

speeds in excess of 10 m/s occurring about 10-20 times per year (Birnbaum et al., 2010; Reijmer and van den Broeke, 2003). Only few precipitation events, introduced by low pressure systems, bring most of the annual precipitation amount (Schlosser et al., 2010; Reijmer and van den Broeke, 2003; Noone et al., 1999). Average accumulation rates over the past 200 years have been ∼60 mm w.eq. (Oerter et al., 2000), possibly with a considerable increase during the last ~~100 years~~ century (Medley and Thomas, 2019). The snow surface around Kohnen Station is mainly comprised of small dunes and sastrugi with horizontal scales of the order of a few metres (Birnbaum et al., 2010).

2.2 Snow core sampling

A set of snow profiles was sampled in December 2018 at ~~various sites along the~~ six sites along a ∼120 km transect south-west of Kohnen Station (Fig. 1a). At each of ~~the six~~ these sampling sites (D2, C4, C5, D7, D24 and D38) we extracted five 1 m snow cores along a line running perpendicularly to the dominant large scale wind direction, with a 10 m interprofile spacing (Fig. 1b). The directionality was chosen to allow a comparison to the studies at the Kohnen trenches (Münch et al., 2016, 2017). As the snow dunes in the study region are predominantly parallel to the wind direction, measuring perpendicular to the wind ensures to better sample the dunes along the 60 m overall distance. Each snow profile was extracted by vertically inserting a 1 m carbon fibre pipe into the sidewall of a snow-pit. At Kohnen Station, the collected snow profiles were cut horizontally into 1.1 cm (the upper 16.5 cm) and 3.3 cm (the lower part) slices, accounting for the diffusion length of ∼3 cm at 1 m depth (Laepple et al., 2018). ~~Due to small compression and expansion errors~~ Compression or expansion during handling, transporting ~~, and cutting , this resulted in 41 to 43~~ and cutting the snow cores resulted in a maximum depth uncertainty of 2 cm and slight variations (41-43) in the number of samples per profile~~, which led us to assume a maximum depth uncertainty of 2~~. Combined with the maximum uncertainty of 1 cm resulting from the snow height measurements (Sect. 2.6), the absolute depths values have a combined maximum uncertainty of 3 cm. All ~~cut~~ snow samples (N = 1249) were packed in plastic bags and transported in a frozen state to Germany for further analysis.

2.3 Stable water isotope measurements

The stable water isotopic composition (δ^{18}O, δD) of the snow samples was measured using a Cavity Ring-Down Spectroscopy instrument ~~(CRDS)~~ of PICARRO Inc. (model L2140-i) in the Stable Isotope Facility at the ~~Alfred Wegener Institute~~ Alfred-Wegener-Institute in Potsdam, Germany~~, applying post-run corrections~~. Post-run corrections were applied as described in Münch et al. (2016). Scaling to the VSMOW/SLAP (Vienna Standard Mean Ocean Water/Standard Light Antarctic Precipitation) scale results in the δ-notation which describes the ratio of heavy to light isotopes in ‰. In-house standards were used for quality control. The mean combined measurement uncertainty is 0.07 ‰ for δ^{18}O and 0.5 ‰ for δD (root-mean-square deviation, RMSD). In the following we focus on the δ^{18}O values.

Table 1. Summary of the datasets which are used within this study. Subgroups of the Kohnen trenches, described in Sect. 2.4, are used to compare the resulting signal to noise ratios (SNRs) to the ones of locations D2, C4, C5, D7, D24 and D38.

Site	Sampling time	Spacing [m]	Depth [m]	Resolution [cm]	number of profiles	SNR subgroups
D2, C4, C5, D7, D24, D38	Dec. 2018	10	1	1.1 - 3.3	5 each	-
Trench t13.1[a]	2012/13	0.1 - 2.5	1.2	3	38	5
Trench t13.2[a]	2012/13	∼ 10-20	1.2	3	4	1
Trench t15.1[b]	2014/15	5	3.4	3	11	2
Trench t15.2[b]	2014/15	5	3.4	3	11	2

[a] Münch et al. (2016), [b] Münch et al. (2017)

2.4 Trench isotope subset

To complement the datasets from the six sites along the transect, we use already published δ^{18}O profiles from Kohnen Station (Fig. 1a) derived in the years 2012/13 and 2014/15 by Münch et al. (2016, 2017). Four snow trenches, in the following called Kohnen trenches, were excavated by a snow blower perpendicularly to the local snow dune direction. Snow profile samples were collected off the trench walls, resulting in snow profiles of high vertical as well as horizontal resolutions (Table 1). For the comparison of the trench data to the new datasets, we divided the trench data into 10 subgroups, each composed of four to five one metre deep δ^{18}O profiles at distances of 10 ± 1 m from one another (Table 1).

2.5 Definition and quantification of stratigraphic noise

~~We define stratigraphic noise as the fraction of the isotope records that differs between adjacent profiles~~The variations that are independent between adjacent isotope records are considered to be noise, while the signal is the isotope variations that those ~~profiles~~ records have in common. The relative ratio of the common (signal variance) to the independent (noise variance) portion in the given data is the ~~so-called~~ signal to noise ratio (SNR). This ratio can be derived based on the pairwise correlation coefficient, r_{XY}, between two isotope profiles X and Y, with

$$SNR_{XY} = \frac{r_{XY}}{1 - r_{XY}} \tag{1}$$

(Fisher et al., 1985). In the absence of any noise, we would expect $r_{XY} = 1$, i.e., a perfectly stratified isotopic imprint. As the amount of stratigraphic noise increases, the pairwise correlations and hence the SNRs will decrease. SNR thus provides a quantitative measure allowing us to objectively determine the proportion of stratigraphic noise in adjacent (intrasite) isotope records and to make intersite comparisons. At each ~~new~~ sampling site, SNRs were estimated based on the average pairwise correlation coefficient (n = 10) between the five δ^{18}O profiles (linearly interpolated to a 0.1 mm resolution) at their absolute height reference (Appendix ~~A~~A). The SNR of the Kohnen trenches was determined as the mean of all pairwise correlations of all subgroups (n = 95). Due to statistical uncertainty, SNR estimates can be negative; as this has no physical meaning, SNR estimates of < 0 are set to 0. ~~In addition, we~~ We employ bootstrap resampling to ~~further~~ assess the uncertainty of the SNR

estimates. ~~With this approach, ~~: we resample the pairwise correlation coefficients with replacement, calculate the SNR from the resamples, and derive the confidence intervals from the distribution of SNRs.

2.6 Environmental properties

The amount of stratigraphic noise in the isotope records is compared to the local slope inclination, accumulation rate, and surface roughness.

Slope inclinations are hereby defined as the local inclination along 10 km down the transect (azimuth of $\sim$57.1°). They were derived using 200 m resolution data from the REMA digital elevation model (DEM, Howat et al., 2019) and vary between 0.3 and 3.1 m km^{-1}.

We use the average accumulation rates over the last 200 years as determined by Rotschky et al. (2004) for the same transect using ice-penetrating radar. ~~This data showed that accumulation rates at ~~For sites D2, D7, D24, and D38~~varied~~, they vary between $\sim$43 and $\sim$59 mm w.eq. a^{-1} ~~. At Kohnen Station, the corresponding value is ~~and compare to $\sim$64 mm w.eq. a^{-1} at Kohnen Station (EPICA community members, 2006).

Snow heights were measured with a 2 m horizontal resolution and a height accuracy of $\pm$1 cm along the line of the five snow cores at each site (60 m length; cf., Fig. 1b) using a Geodät levelling device. Surface roughness is defined by the standard deviation SD$_{\overline{sh}\ SH}$ of these surface heights. To assess past snow surface heights and roughnesses, common isotopic extremes, i.e., isochrones, were ~~assigned and ~~manually traced wherever possible.

3 Results

3.1 δ^{18}O profiles

Mean δ^{18}O values at the new sampling sites range from -43.9 ‰ to -44.3 ‰ (Table 2, Fig. 2) with no significant differences between sites (two-sided Student t-Test; p > 0.05). The mean vertical variance within the arrays of the isotope profiles is σ^2 = 8.9 ‰^{2} (SD 2.9 ‰^{2}) and thus slightly higher than the mean horizontal variance of σ^2 = 7.5 ‰^{2} (SD 5.5 ‰^{2}). Between 4 and 9 local δ^{18}O maxima were observed in the isotope profiles (Fig. 2) with a mean peak to peak amplitude of 5.0 ‰ (SD 3.0 ‰).

3.2 Recent and past snow surfaces and surface roughnesses

The surface roughness ~~, defined by the standard deviation SD$_{sh}$ of the surface heights, ~~SD$_{SH}$ varies between 3.5 cm (Kohnen trenches) and 8.6 cm (D24) (Table 2). The variations at the Kohnen trench site are significantly smaller compared to the other sites (two-sided ~~f-Test~~F-test, p < 0.05). Sites D24, D7, and C4 as well as sites D2, C5, and D38 form two distinct clusters, with no significant intracluster differences in surface roughness, but ~~considerable ~~significant intercluster variations.

At two sites (D2 and D38), it was possible to tentatively trace past snow surface variations by manually tracking local isotope extremes, i.e., isochrones (Fig. 2). This ~~could also be ~~was also done, with a high degree of confidence, at two of the Kohnen trenches (~~13.1 and 13.2~~t13.1 and t13.2; Table 1) by Münch et al. (2016). In contrast, the ~~assignation ~~assignment of common
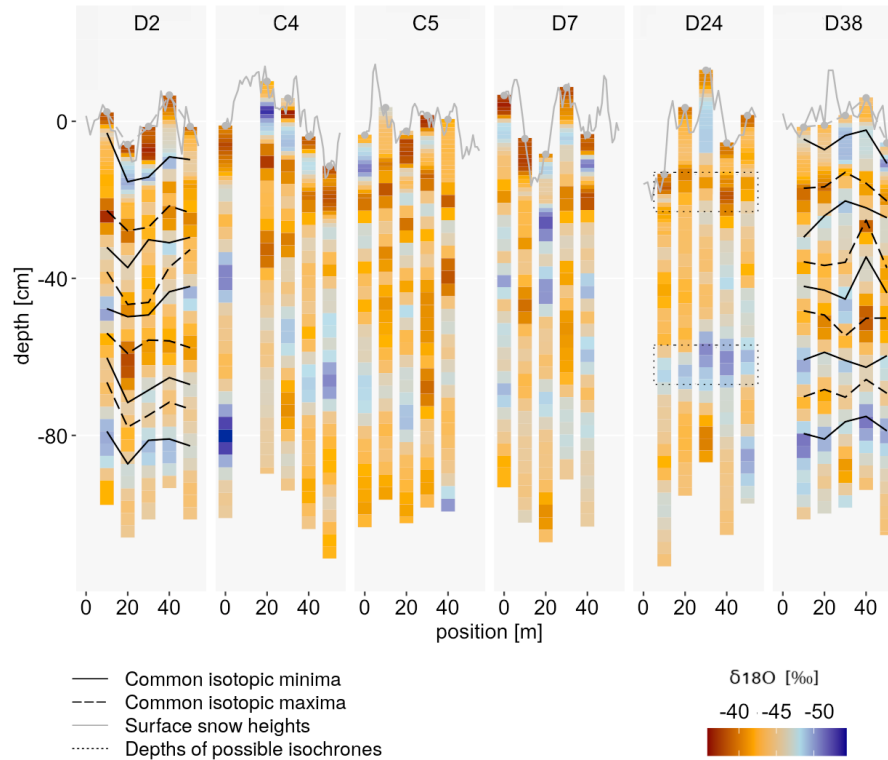
Figure 2. δ^{18}O profiles at each of the new sampling sites plotted against snow depth. The colour scale shows the δ^{18}O values. Black lines trace possible common isotope minima (solid lines) and maxima (dashed lines), wherever it was possible to identify common peaks (sites D2 and D38). Grey lines indicate the surface topography at 2 m (solid line) and 10 m (dashed line) horizontal resolutions. The black dashed boxes at site D24 indicate the depths of similar isotopic peaks, even if consecutive isochrones could not be assigned.

peaks was more ambiguous and uncertain at site D38 and particularly at D2 where one to two cycles might have been missed in the top 25 cm.

At all three sites ,~(D38, D2 and Kohnen), the isochrones (black horizontal lines in Fig. 2) exhibit a similar degree of roughness (SD$_{past}$) as the snow surface (grey dashed lines in Fig. 2) with SD$_{surface}$ = 3 cm and SD$_{past}$ = 3.7 cm at the Kohnen trenches (Münch et al., 2016), SD$_{surface}$ = 3.7 cm and SD$_{past}$ = 3.5 cm at D2, and SD$_{surface}$ = 4 cm, SD$_{past}$ = 3.4 cm at D38. At ~~site~~ D2, ~~certain surface features may have been preserved over several years resulting in~~ correlation coefficients between isochrone profiles and the surface heights (grey dashed lines, Fig. 2) ~~of between~~ range from 0.47 ~~and~~ to 0.87, which suggests that the topography might have been preserved over the years. At site D38, the same test results in correlation coefficients between -0.79 and 0.90, indicating an annual reorganisation of the stratigraphy which ~~are~~ is consistent with earlier findings at the Kohnen trenches (Münch et al., 2016).

At site D24, ~~equally strong isotopic values~~ strong isotopic anomalies were found at depths of about -20 and -60 cm. Depending on the exact ~~depth of the traced~~ choice when tracing these isochrones, the resulting SD$_{past}$ varies between 1 and 2.8 cm,
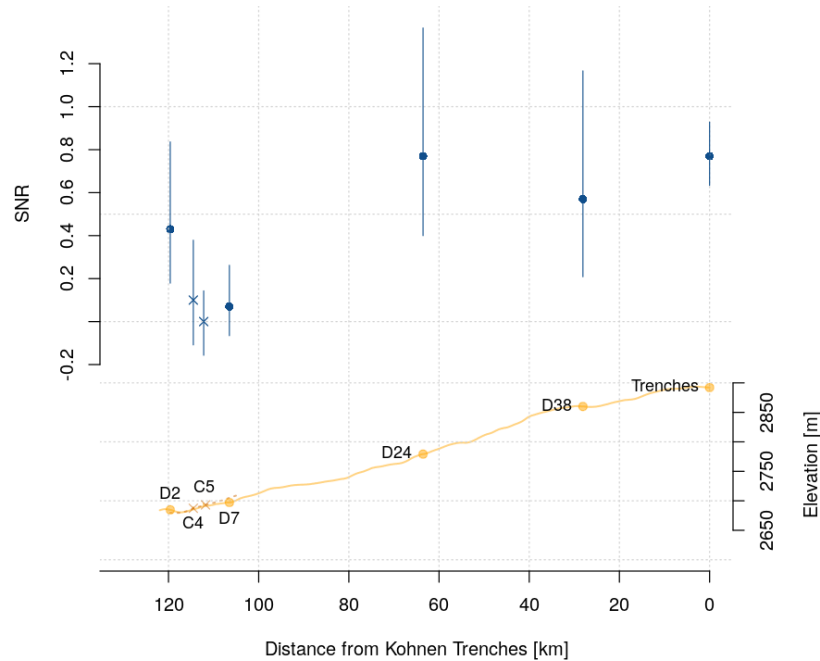
Figure 3. Signal to noise ratio (SNR) and the 95% confidence intervals (blue lines) at the different sites (top panel) and their positions along the transect (bottom panel) with elevations from the RAMP2 DEM (yellow line, Liu et al., 2015). The elevation data at C4 and C5 was collected along a transect that was slightly (~~several~~ $\sim$ 7 km) offset to the north.

which differs significantly from the $\text{SD}_{surface}$ of 10 cm. However, as for sites C4, C5, and D7, consecutive δ^{18}O isochrones at D24 could not be traced with sufficient confidence due to strong irregularities in the isotopic cycles.

3.3 Signal to noise ratios

~~The SNRs provide an estimate of stratigraphic noise imprinted in the δ^{18}O profiles (Fig. 3 and Table 2). We estimated them for each of the newly sampled sites and for the Kohnen trenches. Overall, the SNRs~~ SNRs range from 0 (C5) to 0.77 (Kohnen trenches and D24) ~~.~~ (Fig. 3 and Table 2). The statistical uncertainty of SNR estimates is lower at sites with low SNRs (C4, C5, D7) as well as at the Kohnen trenches~~, which is due to the higher amount~~. For the latter, this is caused by the higher amounts of δ^{18}O profiles available. The highest uncertainty was estimated for sites D38 and D24. Considering these uncertainties, the SNR at the Kohnen trenches is statistically significantly ~~elevated~~ higher (p < 0.05) compared to C4, C5 and D7. Furthermore, the SNR at D24 is significantly higher than at C5 and D7 while the SNR at D2 is significantly higher than at C5.

Table 2. Summary of the isotopic and environmental parameters for all sampling sites showing $\delta^{18}O$ [‰] and their standard deviations $SD_{\delta^{18}O}$, signal to noise ratios (SNRs), mean accumulation rates (A) derived from ground penetrating radar (Rotschky et al., 2004) in water equivalent [mm w.eq. a^{-1}] and snow equivalent [cm snow a^{-1}], surface roughness (SD_{SH} [cm]), the maximum height difference between two local/adjacent snow cores [cm] and slope inclinations [m km^{-1}]. For converting accumulation rates from water equivalent to snow equivalent we assumed a snow density of 344 kg/m^3, which is the overall arithmetic mean for all sites (n = 19).

Site	$\delta^{18}O$ [‰]	$SD_{\delta^{18}O}$ [‰]	SNR	A [mm w.eq. a^{-1}]	A [cm snow a-1]	SD_{SH} [cm]	Max. height difference [cm]	Slope [m km^{-1}]
D2	-44.1	3.0	0.43	58.7	20.2	4.75	12.6	0.55
C4	-44.6	3.3	0.10	-	-	7.23	11.3	1.84
C5	-43.5	2.7	0	-	-	5.50	7.0	2.22
D7	-44.6	2.9	0.07	43.6	15.0	7.35	17.0	1.97
D24	-44.7	2.7	0.77	43.3	14.9	8.55	26.5	3.12
D38	-45.2	2.9	0.57	52.8	18.1	5.36	7.5	0.35
~~Trenches~~Kohnen trenches	-44.7	3.1	0.77	64.0	22.0	3.47	15.5	0.59

4 Discussion

We found ~~different isotopic structures and different amounts~~ strong variations in the amount of stratigraphic noise ~~within replicate 1 m isotope records from seven different sites across a~~ between the seven sites on the 120 km transect~~, coupled with~~. The sites are also characterised by differing snow surface features, slope inclinations, accumulation rates and surface roughnesses. In this section, we discuss the observed differences and possible relationships, and conclude ~~some~~ recommendations for future studies.

4.1 Isotope profiles and snow height evolution related to sastrugi and glazed surfaces

In shallow isotope profiles, which are not yet superimposed by diffusion (Laepple et al., 2018), $\delta^{18}O$ minima represent snow that fell at colder atmospheric temperatures, i.e., in austral winter, while the maxima represent warmer temperatures from summer (e.g., Stenni et al., 2016; Dansgaard, 1964). Common ~~isotope~~ isotopic peaks are therefore assumed to represent snow which accumulated during the same season or even ~~during~~ the same accumulation event. Within these estimated isochrones, the isotope values between the snow cores show some variations. Isotope values within isochrones at location D2 and D38 have a mean SD of 1.6 ‰. Such variations can be expected within the same season (e.g., summer or winter). They also result from isotopic diffusion, as the thickness of a snow layer with a certain isotopic values will affect how much the amplitude is reduced.

Based on the accumulation rate estimates ~~by Rotschky et al. (2004)~~(Rotschky et al., 2004), we expect the 1 metre profiles to have accumulated within ∼4.5 to ∼6.7 years, and to exhibit an equal number of isotopic maxima and minima if from the same
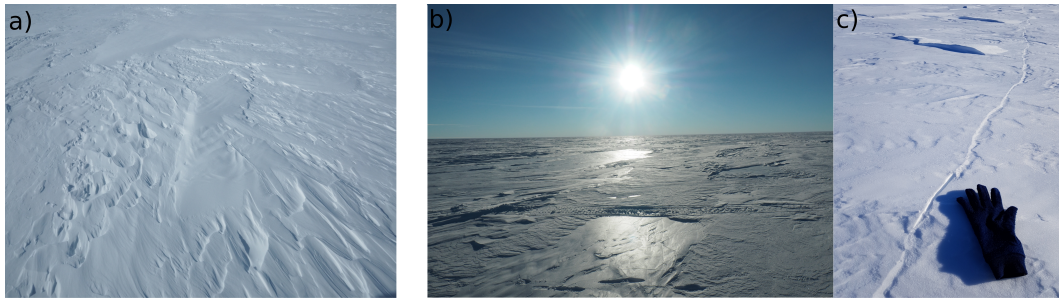
Figure 4. The snow surface at sites a) C4 showing the typical sastrugi, b) D24 showing a mix of sastrugi and glazed surfaces, and c) D24 showing a "thermal" crack with a glove placed next to it for scale.

185   site. However, the absolute count of isotopic peaks varied considerably~~between~~, also between adjacent profiles. Furthermore, the isotope profiles exhibited strongly varying cycle lengths and amplitudes which made it difficult to assign common isotopic peaks and which suggests a considerable redistribution and irregular accumulation. This is further confirmed by the analysis of the evolution of snow heights at D2 and D38. Particularly at D38 a refilling of troughs combined with a lower accumulation at elevated parts show typical processes of snow deposition (Zuhr et al., 2021). At D2, D38 and the Kohnen trenches, the surface

190   snow heights (grey solid lines in Fig. 2) show similar variations as past snow heights, indicating similar surface roughnesses over time. Furthermore, these variations indicate the presence of pronounced snow features such as dunes (Birnbaum et al., 2010).

     The highest surface roughness was observed at site D24, where isotopic peaks were too variable to assign consecutive isochrones. Still, similar isotopic values indicate a very low surface roughness at depths of around -20 and -60 cm. These

195   nearly flat past surfaces are consistent with observed snow surface features around the site, namely glazed surfaces between patches of large sastrugi and dunes ~~mixed with glazed surfaces~~ (Fig. 4a). ~~The latter are characterised~~ Glazed surfaces are characterized by flat and very dense snow, permeated by "thermal" cracks (Fig. 4b and c, e.g., Furukawa et al., 1996). Glazed surfaces were found to occur when high wind speeds coincide with a hiatus in accumulation, e.g., on the steep slopes in the katabatic wind region (Scambos et al., 2012; Furukawa et al., 1996) and could already be detected via satellite images within

200   ∼200 km to the south, south-east, and north-west of the transect (Rotschky et al., 2006).

4.2   Amount and structure of stratigraphic noise

~~In~~ For the newly collected isotope profiles~~we observed a~~, the low mean pairwise correlation coefficient of r = 0.19 (SD 0.31) ~~which is already an indication of~~ indicates strong stratigraphic redistribution and irregular deposition. The pairwise correlations were ~~furthermore~~ independent of the spatial distance between profiles (Appendix ~~C~~B), which confirms that the decorrelation

205   length of stratigraphic noise in the study area is < 10 m as proposed by Münch et al. (2016) for Kohnen Station. The SNRs of < 1 indicate that stratigraphic noise explains more than 50% of the δ^{18}O variability in the uppermost 1 m at all sites, which is consistent with previous findings for this region and confirms the low representativity of single isotope profiles (Münch et al.,
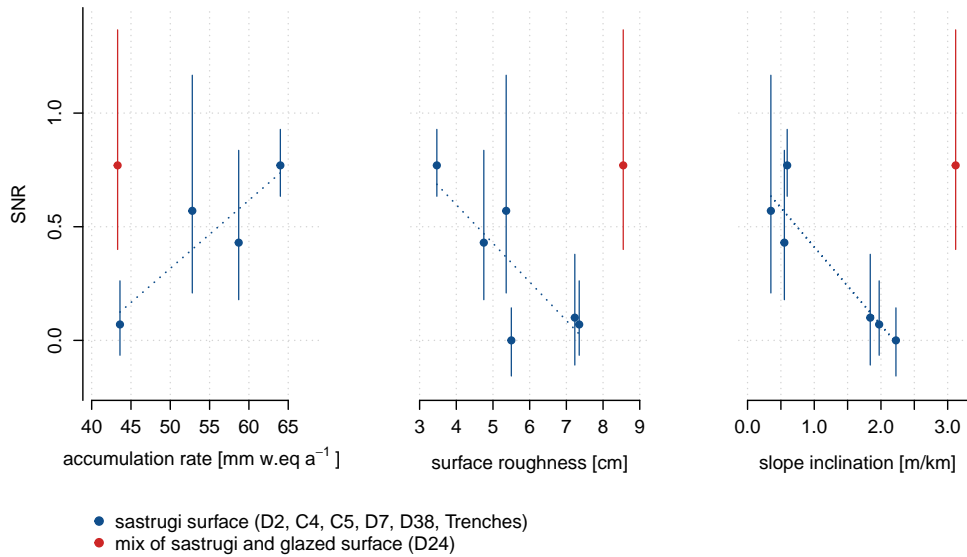
Figure 5. Comparison of signal to noise ratios (SNR) to accumulation rate A [mm w.e. a^{-1}], surface roughness SD_{SH} [cm], and slope inclination [m km^{-1}]. Most sites were dominated by sastrugi while at D24 we observed a mix of sastrugi and glazed surfaces. The latter was therefore excluded in the linear regression analysis (dashed lines). Vertical lines indicate the 95% confidence intervals of the SNR estimates.

2016, 2017; Graf et al., 2002). Along the 120 km transect, SNRs varied strongly between 0 and 0.77 which emphasises the importance of understanding its drivers.

210 **4.3   Relations between stratigraphic noise and environmental properties**

Despite the low number of data points, ~~we could formulate certain hypotheses~~ the strong variations between sites allow to formulate some hypothesis regarding the origin of stratigraphic noise. ~~We could test whether the amount of stratigraphic noise is related to~~ For this aim, we compare the SNRs with the local environmental characteristics ~~such as local~~ namely accumulation rates, slope inclination, and surface ~~roughness~~ roughnesses (Fig. 5). We exclude spatial variations in precipitation or isotopic

215 amplitudes as factors potentially affecting SNRs (Fisher et al., 1985) as we do not expect these features to differ strongly across the spatial scale considered here (Goursaud et al., 2018; Münch and Laepple, 2018, in Appendix).

At the sites dominated by sastrugi (all except D24; cf., blue points, Fig. 5), ~~we found that SNRs correlated~~ SNRs show a strong positive correlation with accumulation rates (r = 0.89~~), and was anticorrelated with surface roughness~~, p = 0.11) and strong negative correlations with surface roughnesses (r = -0.81, p = 0.05) and slope ~~inclination~~ inclinations (r = -0.92, p <

220 0.05). ~~Concomitantly,~~ This is consistent to earlier findings which showed that isotope records at coastal sites in East Antarctica with higher accumulation rates ~~contained~~ contain a more consistent climate signal than those at lower accumulation sites in

DML (Helsen et al., 2005) or near Dome Fuji (Hoshina et al., 2014). The negative correlation of SNRs and surface roughnesses, thus higher undulations related to more noise, is intuitive. It indicates that, although the surface roughness represents only a snapshot of a single summer season, this snapshot is at least partly representative for the general surface roughness during the past years. If this is confirmed, the surface roughness, which is easy to measure, could be used as an indicator of the stratigraphic noise. The correlation between SNRs and slope inclinations is robust to the spatial scales over which the inclination is calculated (Appendix C).

At D24, past and present surface roughnesses were inconsistent which could be related to the surface consisting of a mix of sastrugi and glazed surfaces, which can alternate both spatially and temporally. This feature was (visually) unique compared to the other sites and coincided with the lowest accumulation rate, the highest slope inclination and the highest surface roughness. The relationships between SNR and environmental properties, as proposed for sites dominated by sastrugi, do not seem to hold up at a site of such extreme environmental properties and the related occurrence of glazed surfaces (e.g., Frezzotti et al., 2002; Furukawa et al., 1996). We speculate that D24 represents a discontinuous record in which the two flat anomalies / isochrones represent a summer and a winter layer from any time within the nearly 7 years of accumulation. The SNR, as defined in this study, is the ratio of the shared signal between the records and the local variations. Therefore, the estimated SNR at site D24 is high, driven by the two anomalies. Between the two anomalies, the past surface roughnesses could have been as high as the present surface roughness. We therefore assume that the spatially coherent part at this site does not represent a seasonal or annual climatic signal and that the isotope records do therefore not provide any useful information for climate signal interpretations.

4.4 Relations between slope inclination, surface roughness, and accumulation rates

We also found strong covariations among the different environmental properties. For instance, surface roughness was higher at sites with higher slope inclinations (r = 0.82, p < 0.05) and smaller accumulation rates (r = -0.97, p < 0.05), while the latter correlates negatively with slope inclinations (r = -0.82, p = 0.09). These findings partly contrast Fisher et al. (1985), who proposed that sastrugi heights would be inversely proportional to accumulation rate in Greenland. Furthermore, Studinger et al. (2020) have questioned the validity of such relationships for large spatial scales. However, close links were frequently confirmed at smaller scales: for example, accumulation rates tend to be lower in areas with steeper slopes in various EAP locations (e.g., Dattler et al., 2019),

often associated with the underlying bedrock topography (e.g., Fujita et al., 2011; Arcone et al., 2005; Eisen et al., 2005; Black and Budd, 1964) or wind driven sublimation (e.g., Frezzotti et al., 2004) and redistribution (King et al., 2004). Steeper slopes are associated with stronger wind speeds (e.g., Dattler et al., 2019; Parish and Cassano, 2003; Broeke and Lipzig, 2003; Whillans, 1975; Endo and Fujiwara, 1973) which in turn affect snow surface features ~~(Furukawa et al., 1996; Whillans, 1975, e.g.,)~~ (e.g., Furukawa et al., 1996; Whillans, 1975). High wind speeds increase both the propagation speed and height of dunes and thereby increase surface roughness (Filhol and Sturm, 2015; Birnbaum et al., 2010; Endo and Fujiwara, 1973), at least within the physical constraints of maximum snow heights (e.g., about 1.5 m for sastrugi, Filhol and Sturm, 2015).

4.5 Implications for future studies and high resolution climate reconstructions

Based on the presented dataset, we conclude that the assessed environmental properties affect the amount of stratigraphic noise. However, due the low number of sampling sites, replicates, and shallow sampling depths the SNR estimates are subject to a considerable uncertainty which renders our results somewhat speculative, even if they are supported by previous studies. Furthermore, ~~considering~~ the significant covariance among the different environmental properties makes it difficult to disentangle their individual contributions. Additional studies, ideally ~~collecting~~ including more replicates and deeper profiles that cover a wider range of depositional conditions, are needed to test and refine the proposed relationships~~.~~: In a first order approximation, an increase of the number of snow cores or the length of cores by factor n will reduce the standard error of the correlations by $1/\sqrt{n}$. That means, increasing the number of cores by factor 4, already decreases the uncertainty of the pairwise correlations by half. Given the significant cost and work associated with collecting samples in situ, it would be useful to test whether high frequency ground penetrating radar (e.g., Studinger et al., 2020; Rotschky et al., 2006) could serve to estimate stratigraphic noise. This would ~~have the added advantage that it could~~ allow to cover much larger spatial scales which would provide information on possible large scale drivers such as precipitation patterns (Fisher et al., 1985). Moreover, ~~surface snow accumulation studies following the approaches of Picard et al. (2019) and Zuhr et al. (2021)~~ continuous monitoring of the snow surface and accumulation using a laser scanner or photogrammetry (Zuhr et al., 2021; Picard et al., 2019) could provide more detailed knowledge about variations in snow stratigraphy related to depositional conditions including wind speeds.

~~Based on the fact that stratigraphic noise varied considerably over relatively small spatial scales (~120 km), making a thorough decision on the drilling locations can result in a strong improvement of the isotopic signal within snow or firn cores. In general, areas with reduced slope inclinations, lower surface roughness, and higher accumulation rates are better suited to derive a high resolution climate signal.~~ While data on small scale accumulation rates (Rotschky et al., 2004) and surface roughnesses (e.g., Studinger et al., 2020) are scarce, slope inclination data are available at high spatial resolutions for the entire Antarctic (e.g., Howat et al., 2019) and can easily be used for site selection. We assume that areas ~~characterised~~ characterized by glazed surfaces are poorly suited sampling locations, as ~~they don't exhibit a strong climate signal~~ the archival of the climate signal might be intermittent. Such locations can be excluded by in situ observations, by employing remote sensing approaches to snow surface classification (Scambos et al., 2012; Rotschky et al., 2006) or selecting locations with low slope inclinations and a certain amount of accumulation (e.g., Furukawa et al., 1996).

We suggest that an optimal site selection might allow to increase the effective resolution of climate reconstructions from the
290 East Antarctic Plateau. As the stratigraphic noise considerably varies over relatively small spatial scales (~100km), the optimal choice of a drilling location can minimise the stratigraphic noise and thus improve the SNRs within snow or firn cores. In most cases, the SNR and not the measurement resolution is the limiting factor for the temporal resolution of the climate signal that can be recovered (Münch and Laepple, 2018). The higher the noise level, the more averaging in time is needed to reduce the uncorrelated (white) noise while preserving the more persistent (red) climate signal. As an example, when assuming a climate
295 signal with a Power Spectral Density = f^{-beta}, with beta = 1, and uncorrelated noise, a reduction of the noise by a factor of n would increase the obtainable climate resolution by the same factor. Assuming that 50 % of the noise is stratigraphic noise (Laepple et al., 2018), we would expect up to four times the obtainable climate resolution at Kohnen (SNR of 0.77) relative to C4 (SNR = 0.1).

Considering that the ice sheet topography ~~is proposed to have been~~ was fairly constant over large parts of the EAP during
300 the past millennium, related to the bedrock topography (Eisen et al., 2005; Steinhage et al., 1999), we ~~can~~ hypothesise that the amount of stratigraphic noise imprinted in the snow over the past decade is representative for past centuries. This could be tested by collecting and analysing long (e.g., 100 m) high resolution firn cores. Furthermore, future studies should account for the fact that ice properties such as stratigraphic noise are advected horizontally due to ice flow (Arcone et al., 2005; Steinhage et al., 1999) by checking for similarly suitable environmental properties further upstream. The size of that area can be determined
305 based on ice flow velocity (e.g., Rignot et al., 2019; Arthern et al., 2015) and desired snow or firn core length. With such a sampling strategy, the results presented here can serve to derive a less noisy isotope signal from firn cores~~of probably hundreds of metres of length.~~, and to increase the resolution of late Holocene Antarctic climate reconstructions.

5   Conclusions

In this work, we assessed stratigraphic noise and its spatial variations along a ~~transect extending for about~~ 120 km transect to the
310 south-west of Kohnen Station, Dronning Maud Land, East Antarctic Plateau. We analysed the local, non climatic variability in δ^{18}O composition at high vertical resolutions across spatial scales ranging from local (60 m) to regional (~~–~~~120 km), assessing its dependency on local environmental properties like accumulation rate, surface roughness, and slope inclination. Within the study area, we found that stratigraphic noise dominated the seasonal to interannual isotopic signal~~, with high spatial variations.~~. The amount of noise also varied significantly across the different sites. At sites that were dominated by
315 sastrugi, stratigraphic noise was lower if the terrain was flatter, the surface less rough, and accumulation rates higher. All these environmental characteristics are typically associated with lower wind speeds. ~~The combination of them is likely to make a site~~ Sites characterised by these properties are likely more suitable for collecting isotope profiles ~~from which~~ that provide meaningful climate signals~~can be extracted. Considering~~. Assuming that the proposed relationships ~~seem to be~~ are stationary over time, these findings could be applied to snow, firn, and ice cores that are several hundred metres in length, and thus ~~greatly~~
320 ~~expand the usage of high resolution isotope records~~ increase the effective resolution of late Holocene climate reconstructions from the East Antarctic Plateau.

Data availability. All measurements are available in the PANGAEA database under doi.pangaea.de/10.1594/PANGAEA.956273 (Hirsch et al. 2023) and doi.pangaea.de/10.1594/PANGAEA.956663 (Laepple et al., 2023)

Appendix A: Height reference

325 When assuming the snow surface to stay similar regarding its height variations, i.e., dunes structures, during the time of snow deposition, snow samples are processed at relative depth to each other, which is done e.g., for surface snow samples and shallow cores (e.g., Casado et al., 2016; Steen-Larsen et al., 2014). If the surface height variations are expected to have changed throughout the time of accumulation, snow cores are instead processed at absolute heights, which was decided for the Kohnen trenches (Münch et al., 2016, 2017). We tested this method for the new dataset, by calculating pairwise correlation

330 coefficients for all possible pairs of isotope profiles at each site (Fig. A1), using both the absolute and relative heights. We would expect the correlation to be stronger with more common signal located at a similar depth, either at absolute or relative heights. We obtained a mean correlation coefficient of r = 0.19 (SD 0.31) when using absolute heights and 0.17 (SD 0.32) for
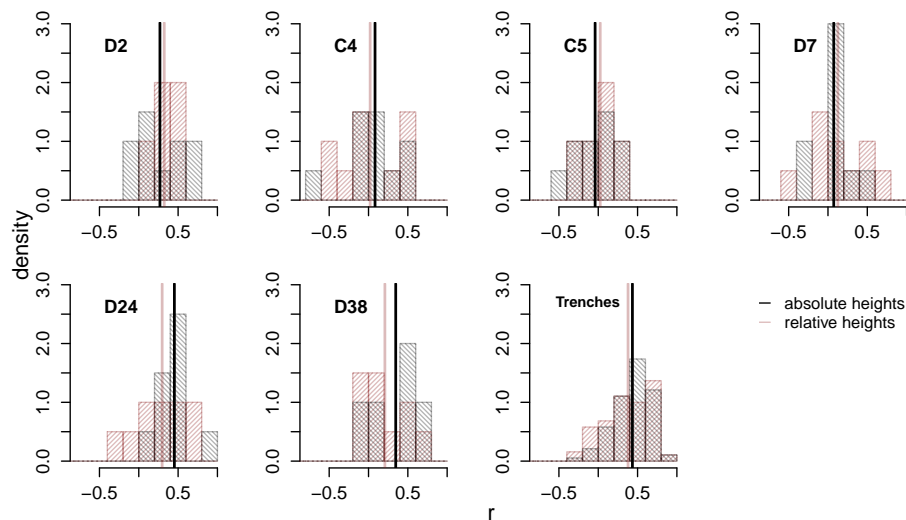
Figure A1. Pairwise correlation coefficients, r, of isotope profiles from different sites using absolute (black) and relative heights (red). Vertical lines show the mean correlation coefficients.

relative heights. The difference of the mean correlations was statistically not significant for any of the sites (p < 0.05, Fig. A1). Additionally, we were unable to identify common isotopic peaks at most sites, which also indicates that local snow heights

335 generally changed fast. At the same time, we were able to confirm highly irregular snow accumulations e.g., at site D38. These

findings are consistent with previous findings (e.g., Münch et al., 2016; Birnbaum et al., 2010). The snow cores in this study are therefore processed at absolute height reference.

Appendix B: Pairwise correlations with inter-profile spacing

Pairwise correlation coefficients for isotope profiles collected at Kohnen Station were found to increase as the interprofile spacing drops to below 5-10 m (Münch et al., 2016), indicating that less distant isotope profiles contain more dependent noise, probably due to the spatial scales of snow surface features like sastrugi. In order to quantify independent noise, we used a minimum interprofile spacing of 10 m in this study. With this setup, we did not find any relationship between spacing and pairwise correlation coefficients (Fig. B1), which indicates that the decorrelation length of stratigraphic noise which was found to be 5 - 10 m at Kohnen station is valid for larger areas across the plateau of DML.
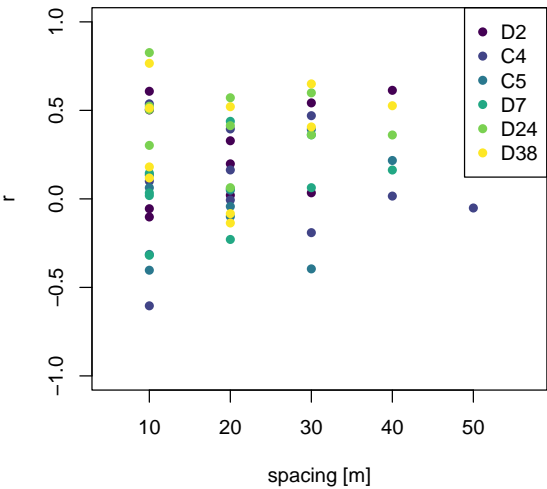
Figure B1. Pairwise correlation coefficients, r, of the δ^{18}O profiles as a function of their interprofile spacing. Colours indicate the different sites.

Appendix C: Slope inclination scales

We calculated slope inclinations for scales ranging from 1 to 15 km (REMA DEM, Howat et al., 2019) and tested how this affected their relations with SNRs, surface roughnesses, and accumulation rates. For SNRs, the absolute values of the correlation coefficient varied slightly for different spatial scales used to calculate slope inclinations, hereby increasing from r = -0.82 (p < 0.05) at 1 km to r = -0.95 (p < 0.05) at 15 km (Fig. C1). A similar strengthening of the correlation with increasing

350 spatial scale was obtained for surface roughness and accumulation rates. Previous studies already proposed the existence of relationships between accumulation rates, slope inclinations and snow surface features for slopes calculated at scales of 1-2 km (Eisen et al., 2005; Arcone et al., 2005; Frezzotti et al., 2002; Furukawa et al., 1996, e.g.,) and 16 km (Black and Budd, 1964). While a link between wind speed and slope inclination has been ~~for~~ established using coarse datasets (e.g., Broeke and Lipzig, 2003; Endo and Fujiwara, 1973; Mather and Miller, 1966) this link was expected to break down with higher resolutions

355 (e.g., 50 km, Kikuchi and Ageta, 1989). Others proposed that small slope changes at scales < 10 km and the commensurate changes in wind speed would be able to explain differences in accumulation rates (Lenaerts et al., 2012), e.g., by sublimation (Frezzotti et al., 2004) and redistribution (King et al., 2004), as well as snow surface features (Whillans, 1975). In this study, we found that correlation coefficients between SNRs, accumulation rates, and surface roughness increased with increasing spatial scales. Yet considering the small size of our sample, the sensitivity of the correlation coefficients to different slope scales could

360 ~~however~~ be dependent on a single surface undulation in the sampling area. We therefore take into account earlier results from wind simulations (e.g., Lenaerts et al., 2012; Whillans, 1975) and variations of accumulation rates and surface features across smaller scales (e.g., Eisen et al., 2005; Arcone et al., 2005; Furukawa et al., 1996; Frezzotti et al., 2002) and ~~therefore~~ do not exceed 10 km for calculating slope inclinations.
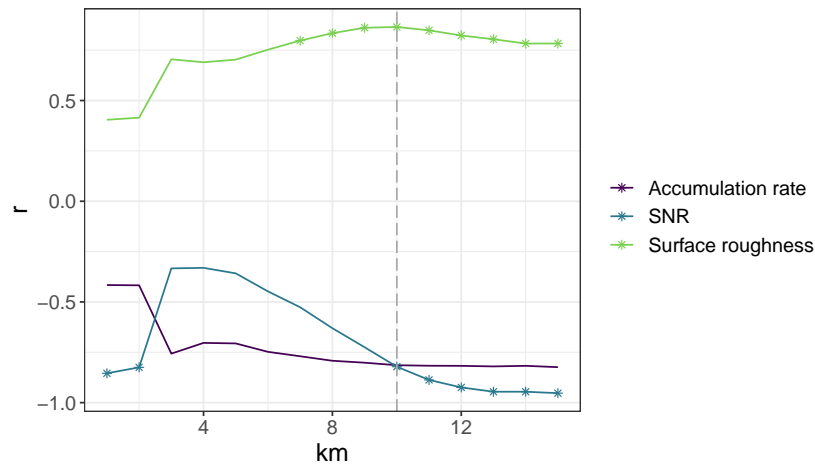
Figure C1. Correlation coefficients, r, between SNRs, surface roughness (SD~~sh~~$_{SH}$), and accumulation rates (A) with slope inclinations calculated using different scales (1-15 km). Stars indicate values with statistical significance (p < 0.05).

Appendix D: ~~**Pairwise correlations with inter-profile spacing**~~

365 ~~Pairwise correlation coefficients for isotope profiles collected at Kohnen Station were found to increase as the interprofile spacing drops to below 5-10 m (Münch et al., 2016), indicating that less distant isotope profiles contain more dependent noise, probably due to the spatial scales of snow surface features like sastrugi. In order quantify independent noise, we used a minimum interprofile spacing of 10 m in this study. With this setup, we did not find any relationship between spacing and~~

pairwise correlation coefficients (Fig. B1), which indicates that the decorrelation length of stratigraphic noise which was found

370   to be 5 - 10 m at Kohnen station is valid for larger areas in DML.

Pairwise correlation coefficients, r, of the δ^{18}O profiles as a function of their interprofile spacing. Colours indicate the different sites.

Author contributions.   TL, MH, and JF designed the expedition and TL designed the sampling strategy. NH and TL designed the study. JF, RD, TL, and MH carried out the sampling on the EAP. NH conducted the isotope measurements with the help of AZ and TM. All authors,

375   especially TL, AZ, and TM, contributed to the scientific analysis. NH performed the analysis and wrote the manuscript, which was reviewed by all authors.

Competing interests.   The authors declare that they have no conflict of interest.

Acknowledgements.   We thank the scientists, technicians, and support staff at Kohnen Station for their assistance, especially Klaus Trimborn for his skilful support during sample collection. Furthermore, we would like to thank Hanno Meyer and Mikaela Weiner for their work in the

380   isotope laboratory at AWI Potsdam, and Christoph Schneider, for the scientific supervision of the initial draft. Data analysis was performed in R: A Language and Environment for Statistical Computing. The Antarctic map is based on Quantarctica datasets in QGIS, kindly provided by the Norwegian Polar Institute (Matsuoka et al., 2018). This project received financial support from the Helmholtz foundation through the Polar Regions and Coasts in the Changing Earth System (PACES II) programme (COMB-I project) and from the European Research Council (ERC) under the EU's Horizon 2020 Research and Innovation Programme (grant agreement no. 716092). It was furthermore supported by

385   the Informationsinfrastrukturen Grant of the Helmholtz Association as part of the DataHub Earth and Environment.

References

Arcone, S., Spikes, V., and Hamilton, G.: Stratigraphic Variation Within Polar Firn Caused by Differential Accumulation and Ice Flow: Interpretation of a 400 Mhz Short-Pulse Radar Profile from West Antarctica, Journal of Glaciology, 51, 407–422, https://doi.org/10.3189/172756505781829151, 2005.

Arthern, R. J., Hindmarsh, R. C. A., and Williams, C. R.: Flow speed within the Antarctic ice sheet and its controls inferred from satellite observations: FLOW SPEED IN THE ANTARCTIC ICE SHEET, Journal of Geophysical Research: Earth Surface, 120, 1171–1188, https://doi.org/10.1002/2014JF003239, 2015.

Barnes, P. R. F., Wolff, E. W., and Mulvaney, R.: A 44 kyr paleoroughness record of the Antarctic surface, Journal of Geophysical Research: Atmospheres, 111, https://doi.org/10.1029/2005JD006349, _eprint: https://agupubs.onlinelibrary.wiley.com/doi/pdf/10.1029/2005JD006349, 2006.

Birnbaum, G., Freitag, J., Brauner, R., König-Langlo, G., Schulz, E., Kipfstuhl, S., Oerter, H., Reijmer, C. H., Schlosser, E., Faria, S. H., Ries, H., Loose, B., Herber, A., Duda, M. G., Powers, J. G., Manning, K. W., and van den Broeke, M. R.: Strong-wind events and their influence on the formation of snow dunes: observations from Kohnen station, Dronning Maud Land, Antarctica, Journal of Glaciology, 56, 891–902, 2010.

Black, H. P. and Budd, W.: Accumulation in the Region of Wilkes, Wilkes Land, Antarctica, Journal of Glaciology, 5, 3–15, https://doi.org/10.3189/S0022143000028549, publisher: Cambridge University Press, 1964.

Broeke, M. R. v. d. and Lipzig, N. P. M. v.: Factors Controlling the Near-Surface Wind Field in Antarctica, Monthly Weather Review, 131, 733–743, https://doi.org/10.1175/1520-0493(2003)131<0733:FCTNSW>2.0.CO;2, publisher: American Meteorological Society Section: Monthly Weather Review, 2003.

Casado, M., Landais, A., Picard, G., Münch, T., Laepple, T., Stenni, B., Dreossi, G., Ekaykin, A., Arnaud, L., Genthon, C., Touzeau, A., Masson-Delmotte, V., and Jouzel, J.: Archival of the water stable isotope signal in East Antarctic ice cores, The Cryosphere Discuss., https://doi.org/10.5194/tc-2016-263, 2016.

Casado, M., Landais, A., Picard, G., Münch, T., Laepple, T., Stenni, B., Dreossi, G., Ekaykin, A., Arnaud, L., Genthon, C., Touzeau, A., Masson-Delmotte, V., and Jouzel, J.: Archival processes of the water stable isotope signal in East Antarctic ice cores, The Cryosphere, 12, 1745–1766, https://doi.org/10.5194/tc-12-1745-2018, 2018.

Casado, M., Münch, T., and Laepple, T.: Climatic information archived in ice cores: impact of intermittency and diffusion on the recorded isotopic signal in Antarctica, Climate of the Past, 16, 1581–1598, https://doi.org/https://doi.org/10.5194/cp-16-1581-2020, publisher: Copernicus GmbH, 2020.

Dansgaard, W.: Stable isotopes in precipitation, Tellus, 16, 436–468, https://doi.org/10.3402/tellusa.v16i4.8993, 1964.

Dattler, M. E., Lenaerts, J. T. M., and Medley, B.: Significant Spatial Variability in Radar-Derived West Antarctic Accumulation Linked to Surface Winds and Topography, Geophysical Research Letters, 46, 13 126–13 134, https://doi.org/10.1029/2019GL085363, 2019.

Dee, S., Emile-Geay, J., Evans, M. N., Allam, A., Steig, E. J., and Thompson, D. M.: PRYSM: An open-source framework for PRoxY System Modeling, with applications to oxygen-isotope systems, Journal of Advances in Modeling Earth Systems, 7, 1220–1247, https://doi.org/10.1002/2015MS000447, 2015.

Dolman, A. M. and Laepple, T.: Sedproxy: a forward model for sediment-archived climate proxies, Climate of the Past, 14, 1851–1868, https://doi.org/https://doi.org/10.5194/cp-14-1851-2018, 2018.

Eisen, O., Rack, W., Nixdorf, U., and Wilhelms, F.: Characteristics of accumulation around the EPICA deep-drilling site in Dronning Maud Land, Antarctica, Annals of Glaciology, 41, 41–46, 2005.

Endo, Y. and Fujiwara, K.: Characteristics of the snow cover in East Antarctica along the route of the JARE South Pole traverse and factors controlling such characteristics, JARE scientific reports. Ser. C, Earth sciences, 7, 1–38, 1973.

EPICA community members: Eight glacial cycles from an Antarctic ice core, Nature, 429, 623–628, https://doi.org/10.1038/nature02599, 2004.

EPICA community members: One-to-one coupling of glacial climate variability in Greenland and Antarctica, Nature, 444, 195–198, https://doi.org/10.1038/nature05301, 2006.

Filhol, S. and Sturm, M.: Snow bedforms: A review, new data, and a formation model: Snow bedforms: Review and Modeling, Journal of Geophysical Research: Earth Surface, 120, 1645–1669, https://doi.org/10.1002/2015JF003529, 2015.

Fisher, D. A., Reeh, N., and Clausen, H. B.: Stratigraphic Noise in Time Series Derived from Ice Cores, Annals of Glaciology, 7, 76–83, https://doi.org/10.1017/S0260305500005942, 1985.

Frezzotti, M., Gandolfi, S., La Marca, F., and Urbini, S.: Snow dunes and glazed surfaces in Antarctica: new field and remote-sensing data, Annals of Glaciology, 34, 81–88, https://doi.org/10.3189/172756402781817851, 2002.

Frezzotti, M., Pourchet, M., Flora, O., Gandolfi, S., Gay, M., Urbini, S., Vincent, C., Becagli, S., Gragnani, R., Proposito, M., Severi, M., Traversi, R., Udisti, R., and Fily, M.: New estimations of precipitation and surface sublimation in East Antarctica from snow accumulation measurements, Climate Dynamics, 23, 803–813, https://doi.org/10.1007/s00382-004-0462-5, 2004.

Fujita, S., Holmlund, P., Andersson, I., Brown, I., Enomoto, H., Fujii, Y., Fujita, K., Fukui, K., Furukawa, T., Hansson, M., Hara, K., Hoshina, Y., Igarashi, M., Iizuka, Y., Imura, S., Ingvander, S., Karlin, T., Motoyama, H., Nakazawa, F., Oerter, H., Sjöberg, L. E., Sugiyama, S., Surdyk, S., Ström, J., Uemura, R., and Wilhelms, F.: Spatial and temporal variability of snow accumulation rate on the East Antarctic ice divide between Dome Fuji and EPICA DML, The Cryosphere, 5, 1057–1081, https://doi.org/10.5194/tc-5-1057-2011, 2011.

Furukawa, T., Kamiyama, K., and Maen, H.: Snow surface features along the traverse route from the coast to Dome Fuji Station, Queen Maud Land, Antarctica, Proc. NIPR Symp. Polar Meteorol. Glacial., 10, 13–24, 1996.

Goursaud, S., Masson-Delmotte, V., Favier, V., Orsi, A., and Werner, M.: Water stable isotope spatio-temporal variability in Antarctica in 1960–2013: observations and simulations from the ECHAM5-wiso atmospheric general circulation model, Climate of the Past, 14, 923–946, https://doi.org/10.5194/cp-14-923-2018, 2018.

Graf, W., Oerter, H., Reinwarth, O., Stichler, W., Wilhelms, F., Miller, H., and Mulvaney, R.: Stable-isotope records from Dronning Maud Land, Antarctica, Annals of Glaciology, 35, 195–201, 2002.

Helsen, M. M., van de Wal, R. S. W., van den Broeke, M. R., van As, D., Meijer, H. A. J., and Reijmer, C. H.: Oxygen isotope variability in snow from western Dronning Maud Land, Antarctica and its relation to temperature, Tellus B, 57, 423–435, https://doi.org/10.3402/tellusb.v57i5.16563, 2005.

Hoshina, Y., Fujita, K., Nakazawa, F., Iizuka, Y., Miyake, T., Hirabayashi, M., Kuramoto, T., Fujita, S., and Motoyama, H.: Effect of accumulation rate on water stable isotopes of near-surface snow in inland Antarctica, Journal of Geophysical Research: Atmospheres, 119, 274–283, https://doi.org/10.1002/2013JD020771, 2014.

Howat, I. M., Porter, C., Smith, B. E., Noh, M.-J., and Morin, P.: The Reference Elevation Model of Antarctica, The Cryosphere, 13, 665–674, https://doi.org/10.5194/tc-13-665-2019, 2019.

Johnsen, S. J., Clausen, H. B., Cuffey, K. M., Hoffmann, G., Schwander, J., and Creyts, T.: Diffusion of stable isotopes in polar firn and ice: the isotope effect in firn diffusion, in: Physics of Ice Core Records, edited by Hondoh, T., vol. 159, pp. 121–140, Hokkaido University Press, Sapporo, Japan, 2000.

Jones, J. M., Gille, S. T., Goosse, H., Abram, N. J., Canziani, P. O., Charman, D. J., Clem, K. R., Crosta, X., de Lavergne, C., Eisenman, I., England, M. H., Fogt, R. L., Frankcombe, L. M., Marshall, G. J., Masson-Delmotte, V., Morrison, A. K., Orsi, A. J., Raphael, M. N., Renwick, J. A., Schneider, D. P., Simpkins, G. R., Steig, E. J., Stenni, B., Swingedouw, D., and Vance, T. R.: Assessing recent trends in high-latitude Southern Hemisphere surface climate, Nature Climate Change, 6, 917–926, https://doi.org/10.1038/nclimate3103, 2016.

Jones, T. R., White, J. W. C., and Popp, T.: Siple Dome shallow ice cores: a study in coastal dome microclimatology, Climate of the Past, 10, 1253–1267, https://doi.org/10.5194/cp-10-1253-2014, 2014.

Jouzel, J. and Masson-Delmotte, V.: Paleoclimates: what do we learn from deep ice cores?, WIREs Climate Change, 1, 654–669, https://doi.org/10.1002/wcc.72, _eprint: https://onlinelibrary.wiley.com/doi/pdf/10.1002/wcc.72, 2010.

Karlöf, L., Winebrenner, D. P., and Percival, D. B.: How representative is a time series derived from a firn core? A study at a low-accumulation site on the Antarctic plateau, Journal of Geophysical Research, 111, https://doi.org/10.1029/2006JF000552, 2006.

Kikuchi, T. and Ageta, Y.: A preliminary estimate of inertia effects in a bulk model of katabatic wind, Proc. NIPR Symp. Polar Meteorol. Glacial., 2, 61–69, 1989.

King, J. C., Anderson, P., and Vaughan, D. G.: Wind-borne redistribution of snow across an Antarctic ice rise, Journal of Geophysical Research, 109, D11 104, https://doi.org/10.1029/2003JD004361, 2004.

Laepple, T., Werner, M., and Lohmann, G.: Synchronicity of Antarctic temperatures and local solar insolation on orbital timescales, Nature, 471, 91–94, https://doi.org/10.1038/nature09825, 2011.

Laepple, T., Münch, T., and Dolman, A. M.: Inferring past climate variations from proxies: Separating climate and non-climate variability, Past Global Changes Magazine, 25, 140–141, https://doi.org/10.22498/pages.25.3.140, 2017.

Laepple, T., Münch, T., Casado, M., Hoerhold, M., Landais, A., and Kipfstuhl, S.: On the similarity and apparent cycles of isotopic variations in East Antarctic snow pits, The Cryosphere, 12, 169–187, https://doi.org/10.5194/tc-12-169-2018, 2018.

Lenaerts, J. T., Van Den Broeke, M. R., Scarchilli, C., and Agosta, C.: Impact of model resolution on simulated wind, drifting snow and surface mass balance in Terre Adélie, East Antarctica, Journal of Glaciology, 58, 821–829, https://doi.org/10.3189/2012JoG12J020, 2012.

Liu, H., Jezek, K., Li, B., and Zhao, Z.: Radarsat Antarctic Mapping Project Digital Elevation Model, Version 2. Boulder, Colorado USA. NASA National Snow and Ice Data Center Distributed Active Archive Center., https://doi.org/http://dx.doi.org/10.5067/8JKNEW6BFRVD, 2015.

Mather, K. B. and Miller, G. S.: Wind Drainage off the High Plateau of Eastern Antarctica, Nature, 209, 281–284, https://doi.org/10.1038/209281a0, 1966.

Matsuoka, K., Skoglund, A., Roth, G., Tronstad, S., and Melvær, Y.: Quantarctica3, Norwegian Polar Institute., p. e961, https://doi.org/https://doiorg. libezproxy. open. ac. uk/10.21334/npolar, 2018.

McMorrow, A. J., Curran, M. A. J., Van Ommen, T. D., Morgan, V. I., and Allison, I.: Features of meteorological events preserved in a high-resolution Law Dome (East Antarctica) snow pit, Annals of Glaciology, 35, 463–470, 2002.

Medley, B. and Thomas, E. R.: Increased snowfall over the Antarctic Ice Sheet mitigated twentieth-century sea-level rise, Nature Climate Change, 9, 34–39, https://doi.org/10.1038/s41558-018-0356-x, number: 1 Publisher: Nature Publishing Group, 2019.

Münch, T. and Laepple, T.: What climate signal is contained in decadal- to centennial-scale isotope variations from Antarctic ice cores?, Climate of the Past, 14, 2053–2070, https://doi.org/10.5194/cp-14-2053-2018, 2018.

Münch, T., Kipfstuhl, S., Freitag, J., Meyer, H., and Laepple, T.: Oxygen isotopes from two snow trenches from Kohnen Station, Dronning Maud Land, Antarctica from the 2012/13 field season, https://doi.org/10.1594/PANGAEA.861675, 2016.

Münch, T., Kipfstuhl, S., Freitag, J., Meyer, H., and Laepple, T.: Constraints on post-depositional isotope modifications in East Antarctic firn from analysing temporal changes of isotope profiles, The Cryosphere, 11, 2175–2188, https://doi.org/10.5194/tc-11-2175-2017, 2017.

500   Noone, D., Turner, J., and Mulvaney, R.: Atmospheric signals and characteristics of accumulation in Dronning Maud Land, Antarctica, Journal of Geophysical Research: Atmospheres, 104, 19 191–19 211, https://doi.org/10.1029/1999JD900376, 1999.

Oerter, H., Wilhelms, F., Jung-Rothenhäusler, F., Göktas, F., Miller, H., Graf, W., and Sommer, S.: Accumulation rates in Dronning Maud Land, Antarctica, as revealed by dielectric-profiling measurements of shallow firn cores, Annals of Glaciology, 30, 27–34, 2000.

Parish, T. R. and Cassano, J. J.: The Role of Katabatic Winds on the Antarctic Surface Wind Regime, Monthly Weather Review, 131,
505   317–333, https://doi.org/10.1175/1520-0493(2003)131<0317:TROKWO>2.0.CO;2, 2003.

Picard, G., Arnaud, L., Caneill, R., Lefebvre, E., and Lamare, M.: Observation of the process of snow accumulation on the Antarctic Plateau by time lapse laser scanning, The Cryosphere, 13, 1983 – 1999, https://doi.org/https://doi.org/10.5194/tc-13-1983-2019, 2019.

Reijmer, C. H. and van den Broeke, M. R.: Temporal and spatial variability of the surface mass balance in Dronning Maud Land, Antarctica, as derived from automatic weather stations, Journal of Glaciology, 49, 512–520, 2003.

510   Rignot, E., Mouginot, J., Scheuchl, B., van den Broeke, M., van Wessem, M. J., and Morlighem, M.: Four decades of Antarctic Ice Sheet mass balance from 1979–2017, Proceedings of the National Academy of Sciences, 116, 1095–1103, https://doi.org/10.1073/pnas.1812883116, 2019.

Rotschky, G., Eisen, O., Wilhelms, F., Nixdorf, U., and Oerter, H.: Spatial distribution of surface mass balance on Amundsenisen plateau, Antarctica, derived from ice-penetrating radar studies, Annals of Glaciology, 39, 265–270, http://www.ingentaconnect.com/content/igsoc/
515   agl/2004/00000039/00000001/art00041, 2004.

Rotschky, G., Rack, W., Dierking, W., and Oerter, H.: Retrieving Snowpack Properties and Accumulation Estimates From a Combination of SAR and Scatterometer Measurements, IEEE Transcactions on Geosciences and Remote Sensing, 44, 943 – 956, https://doi.org/10.1109/TGRS.2005.862524, 2006.

Scambos, T., Frezzotti, M., Haran, T., Bohlander, J., Lenaerts, J., Van Den Broeke, M., Jezek, K., Long, D., Urbini, S., Farness, K., Neumann,
520   T., Albert, M., and Winther, J.-G.: Extent of low-accumulation 'wind glaze' areas on the East Antarctic plateau: implications for continental ice mass balance, Journal of Glaciology, 58, 633–647, https://doi.org/10.3189/2012JoG11J232, 2012.

Schlosser, E., Manning, K. W., Powers, J. G., Duda, M. G., Birnbaum, G., and Fujita, K.: Characteristics of high-precipitation events in Dronning Maud Land, Antarctica, Journal of Geophysical Research: Atmospheres, 115, D14 107, https://doi.org/10.1029/2009JD013410, 2010.

525   Sommer, S., Wagenbach, D., Mulvaney, R., and Fischer, H.: Glacio-chemical study spanning the past 2 kyr on three ice cores from Dronning Maud Land, Antarctica: 2. Seasonally resolved chemical records, Journal of Geophysical Research: Atmospheres, 105, 29 423–29 433, https://doi.org/10.1029/2000JD900450, 2000.

Steen-Larsen, H. C., Masson-Delmotte, V., Hirabayashi, M., Winkler, R., Satow, K., Prié, F., Bayou, N., Brun, E., Cuffey, K. M., Dahl-Jensen, D., Dumont, M., Guillevic, M., Kipfstuhl, S., Landais, A., Popp, T., Risi, C., Steffen, K., Stenni, B., and Sveinbjörnsdottír, A. E.: What
530   controls the isotopic composition of Greenland surface snow?, Climate of the Past, 10, 377–392, https://doi.org/10.5194/cp-10-377-2014, 2014.

Steinhage, D., Nixdorf, U., Meyer, U., and Miller, H.: New maps of the ice thickness and subglacial topography in Dronning Maud Land, Antarctica, determined by means of airborne radio-echo sounding, Annals of Glaciology, 29, 267–272, https://doi.org/10.3189/172756499781821409, 1999.

535 Stenni, B., Scarchilli, C., Masson-Delmotte, V., Schlosser, E., Ciardini, V., Dreossi, G., Grigioni, P., Bonazza, M., Cagnati, A., Karlicek, D., Risi, C., Udisti, R., and Valt, M.: Three-year monitoring of stable isotopes of precipitation at Concordia Station, East Antarctica, The Cryosphere, 10, 2415–2428, https://doi.org/10.5194/tc-10-2415-2016, 2016.

Stenni, B., Curran, M. A. J., Abram, N. J., Orsi, A., Goursaud, S., Masson-Delmotte, V., Neukom, R., Goosse, H., Divine, D., van Ommen, T., Steig, E. J., Dixon, D. A., Thomas, E. R., Bertler, N. A. N., Isaksson, E., Ekaykin, A., Werner, M., and Frezzotti, M.: Antarctic climate

540 variability on regional and continental scales over the last 2000 years, Climate of the Past, 13, 1609–1634, https://doi.org/10.5194/cp-13-1609-2017, 2017.

Studinger, M., Medley, B. C., Brunt, K. M., Casey, K. A., Kurtz, N. T., Manizade, S. S., Neumann, T. A., and Overly, T. B.: Temporal and spatial variability in surface roughness and accumulation rate around 88° S from repeat airborne geophysical surveys, The Cryosphere, 14, 3287–3308, https://doi.org/10.5194/tc-14-3287-2020, 2020.

545 Town, M. S., Warren, S. G., Walden, V. P., and Waddington, E. D.: Effect of atmospheric water vapor on modification of stable isotopes in near-surface snow on ice sheets, Journal of Geophysical Research, 113, https://doi.org/10.1029/2008JD009852, 2008.

van der Wel, G., Fischer, H., Oerter, H., Meyer, H., and Meijer, H. A. J.: Estimation and calibration of the water isotope differential diffusion length in ice core records, The Cryosphere, 9, 1601–1616, https://doi.org/10.5194/tc-9-1601-2015, 2015.

Vinther, B. M., Jones, P. D., Briffa, K. R., Clausen, H. B., Andersen, K. K., Dahl-Jensen, D., and Johnsen, S. J.: Climatic signals in multiple highly resolved stable isotope records from Greenland, Quaternary Science Reviews, 29, 522–538, https://doi.org/10.1016/j.quascirev.2009.11.002, 2010.

Wahl, S., Steen-Larsen, H. C., Reuder, J., and Hörhold, M.: Quantifying the Stable Water Isotopologue Exchange Between the Snow Surface and Lower Atmosphere by Direct Flux Measurements, Journal of Geophysical Research: Atmospheres, 126, e2020JD034 400, https://doi.org/10.1029/2020JD034400, _eprint: https://onlinelibrary.wiley.com/doi/pdf/10.1029/2020JD034400, 2021.

555 Wesche, C., Weller, R., König-Langlo, G., Fromm, T., Eckstaller, A., Nixdorf, U., and Kohlberg, E.: Neumayer III and Kohnen Station in Antarctica operate by the Alfred Wegener Institute., Journal of large-scale research facilities JLSRF, 2, 85, 2016.

Whillans, I. M.: Effect Of Inversion Winds On Topographic Detail And Mass Balance On Inland Ice Sheets, Journal of Glaciology, 14, 85–90, https://doi.org/10.3189/S0022143000013423, publisher: Cambridge University Press, 1975.

Zuhr, A. M., Münch, T., Steen-Larsen, H. C., Hörhold, M., and Laepple, T.: Local-scale deposition of surface snow on the Greenland ice

560 sheet, The Cryosphere, 15, 4873–4900, https://doi.org/10.5194/tc-15-4873-2021, publisher: Copernicus GmbH, 2021.

References